Proceedings of the ASME 2021
International Design Engineering Technical Conferences and Computers and Information in Engineering Conference
IDETC/CIE2021
August 17-20, 2021, Virtual, Online

DETC2021-71254

INTEGER RATIO SELF-SYNCHRONIZATION IN PAIRS OF LIMIT CYCLE OSCILLATORS

Aditya Bhaskar[1], B. Shayak[1], Alan T. Zehnder[1], Richard H. Rand[1]

[1]Sibley School of Mechanical and Aerospace Engineering, Cornell University, Ithaca, NY 14853, USA

ABSTRACT

The existence of multiple stable states of higher order $m{:}n$ locking in coupled limit cycle oscillators has been studied by prior authors in the context of injection-locking in systems driven by an external periodic force. The current work builds on this concept to study the higher order locking characteristics of pairs of limit cycle oscillators self-synchronizing under coupling forces. To this end we analyze three oscillator systems: Van der Pol oscillators using numerical analysis, a simplified model for MEMS oscillators using numerical analysis as well as perturbation theory, and a full model of thermo-optically driven MEMS oscillators using numerical analysis. For the Van der Pol system, higher order locking is observed for the strongly nonlinear case corresponding to relaxation oscillations and the transition from weak to strong nonlinearity is studied using a parameter sweep. Additionally, coupling of a different nature such as quadratic coupling is also capable of inducing higher order coupling in Van der Pol oscillators. For the MEMS systems with linear coupling, higher order locking is observed when a strong cubic stiffness nonlinearity exists. Devil's staircase-like structures are obtained for the coupling strength-frequency ratio parameter space which suggest overlapping Arnold locking regions for $m{:}n$ locks corresponding to different integers.

Keywords: Higher order locking, $m{:}n$ locking, MEMS oscillators, Coupled limit cycle oscillators

1. INTRODUCTION

Self-synchronization of limit cycle oscillators in the presence of a weak coupling field has a rich body of literature [1,2]. In such systems, typical problems of interest are $1{:}1$ frequency self-synchronization in a network of two or more coupled oscillators and $1{:}1$ frequency entrainment of one or more oscillators to an external periodic force. The problem of $m{:}n$ synchronization, where m and n are integers, is widely studied for systems of limit cycle oscillators that are driven by an external periodic force. Some of the practical implementations of such systems are coupled Boolean phase oscillators [3], optomechanical cavities [4] and spintronic feedback nano-oscillators [5]. Studies on the higher order locking of pulse-coupled oscillators [6] and Josephson junctions [7] reveal the prevalence of $m{:}n$ locking in network of oscillators. A general theory of $m{:}n$ locking in externally driven systems along with specific examples of simple nonlinear oscillators and phase-only Integrate and Fire models is given in [8]. The concept of utilizing nonlinearities in the system to achieve $m{:}n$ locking is demonstrated for the simplest case of phase-only oscillators using the Adler model [2]. The Adler model is a first order phase-only model with a sinusoidal nonlinear term. In this system, non-uniformities in the oscillations i.e. a nonlinear increase in the phase of the oscillation with time, induced by increasing the strength of the sinusoidal term, promotes locking at an $m{:}n$ ratio. Higher order locking in an externally driven system is given in a recent work [9]. Nonlinearities in the system have also been used to achieve intermodal coupling via internal resonance [10].

In the current work, strong nonlinearities in the form of cubic stiffness terms are utilized to achieve a Devil's staircase-like structure in undriven, weakly and linearly coupled MEMS limit cycle oscillators. First, a system of two Van der Pol oscillators is studied for different types of coupling and nonlinearity regimes. The time series, phase portraits, power spectra, and phase evolutions are used to determine the nature of locking. Next, a system of two simplified MEMS oscillators is analyzed numerically as well as using the two-variable expansion method for parameters for which it shows $m{:}n$ locking. Building upon the results from these two models, finally a system of two thermo-optical MEMS oscillators is analyzed for higher order locking and the necessity for the presence of cubic nonlinearities to achieve $m{:}n$ locking is emphasized.

2. VAN DER POL OSCILLATOR SYSTEM

The archetypal self-sustaining oscillator in the literature is the Van der Pol oscillator with a damping term that is modulated with amplitude of oscillation. The equations describing two Van der Pol oscillators frequency-detuned with respect to each other and interacting via linear coupling is given by Eq. (1).

$$\ddot{z}_1 + z_1 - \varepsilon(1 - z_1^2)\dot{z}_1 = \varepsilon\alpha(z_2 - z_1),$$

$$\ddot{z}_2 + \kappa z_2 - \varepsilon(1 - z_2^2)\dot{z}_2 = \varepsilon\alpha(z_1 - z_2). \quad (1)$$

In Eq. (1), z denotes the oscillation variable, κ is the linear stiffness parameter that controls the detuning in the system, ε is a scaling parameter, and α is the bi-directional coupling strength acting between the two oscillators. The scaling parameter determines the effects of nonlinearity in the system; a small value of ε results in quasi-harmonic oscillations of the uncoupled Van der Pol system with an approximately linear phase evolution whereas a high value of ε results in a highly nonlinear system exhibiting relaxation-type limit cycle oscillations. In the literature, relaxation-type oscillators are also sometimes referred to as Integrate and Fire oscillators. A system of weakly-coupled limit cycle oscillators exhibits self-synchronization at a 1: 1 frequency lock for small detuning and sufficiently high coupling strengths. The detuning-coupling parameter space famously consists of tongue-like structures of synchronization called Arnold tongues. We now look at the synchronization characteristics of the system of coupled Van der Pol oscillators at different integer ratios m: n and how these characteristics depend on the nonlinearity in the system and the nature of coupling.

For the first set of numerical calculations, the scaling parameter is fixed at a small value, $\varepsilon = 0.01$, such that the system is weakly nonlinear. The detuning parameter is fixed at $\kappa = 0.26$ such that the computed uncoupled drifting frequencies of the oscillators are $f_1 = 1$ and $f_2 = 0.51$ and are close to a 2: 1 ratio. When linear coupling is used, as given in Eq. (1), we observe via direct numerical integration that the system does not lock at a 2: 1 ratio for any coupling strength.

Next, the nature of coupling is changed to quadratic coupling with the model given by Eq. (2).

$$\begin{aligned}\ddot{z}_1 + z_1 - \varepsilon(1 - z_1^2)\dot{z}_1 &= \varepsilon\alpha(z_2 - z_1)^2,\\ \ddot{z}_2 + \kappa z_2 - \varepsilon(1 - z_2^2)\dot{z}_2 &= \varepsilon\alpha(z_1 - z_2)^2.\end{aligned} \quad (2)$$

For the system given by Eq. (2), a locking at 2: 1 ratio is observed for a coupling strength of $\alpha = 1$ with locked frequencies $f_1 = 1.005$ and $f_2 = 0.502$. The corresponding time series, phase portrait, power spectrum, and phase evolution are given in Fig. (1). The time series is plotted with a sampling rate of 10 samples per unit time and the power spectra, calculated using the discrete Fourier transform, have a resolution of 10^{-4} (1/time units). The numerical integration is done using the *odeint* function in *SciPy*. The instantaneous phase of the signal is computed using the analytic signal obtained from the Hilbert transform. Frequency locking is established by considering the Fourier frequencies corresponding to the dominant peaks in the power spectra. It can be noted that 1: 1 locking is not observed for this system even at higher coupling strengths. The calculations suggest that for weakly nonlinear ($\varepsilon \ll 1$) coupled oscillators, the nature of the coupling can determine the presence of m: n locking.

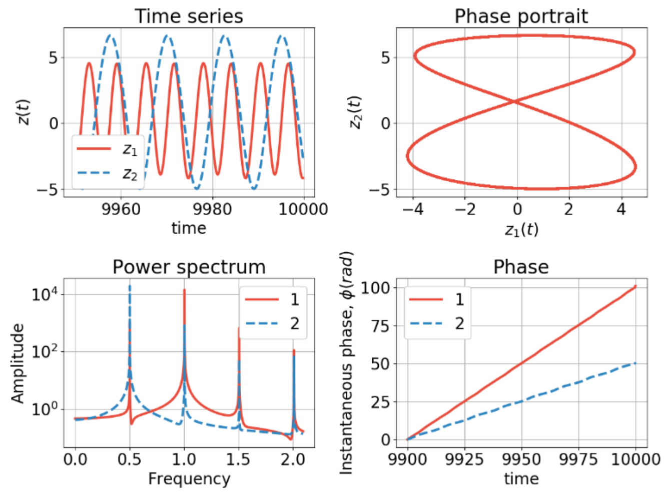

FIGURE 1: 2: 1 locking in a system of two quadratically coupled weakly nonlinear Van der Pol oscillators given by Eq. (2). The time series shows that there are two peaks of the first oscillator for every peak of the second. The phase portrait has a closed loop which implies that the relative motion of the two oscillators is periodic. The frequencies of the oscillators corresponding to the peaks in the power spectrum and the slopes of the instantaneous phase evolution are in the ratio 2: 1.

The system given by Eq. (1) is then studied for a higher value of the scaling parameter $\varepsilon = 10$, which corresponds to a strongly nonlinear system with relaxation oscillations. This implies that there are two distinct time scales in the oscillations, fast time and slow time. The detuning parameter is fixed at $\kappa = 0.26$ such that the uncoupled (drifting) frequencies of the oscillators are $f_1 = 0.33$ and $f_2 = 0.094$. The nature of oscillations for $\alpha = 0.07$ is shown in Fig. (2) and it corresponds to 2:1 locking with frequencies $f_1 = 0.43$ and $f_2 = 0.215$. The non-uniformity in oscillations can be seen in the time series and the phase evolution.

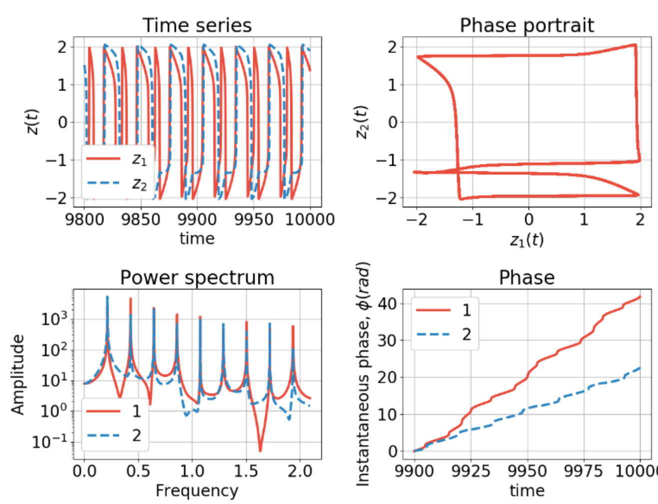

FIGURE 2: 2: 1 locking in a system of two linearly coupled strongly nonlinear Van der Pol oscillators given by Eq. (1). The coupling strength is $\alpha = 0.07$. The locking frequencies are $f_1 = 0.43$ and $f_2 = 0.215$. The time series shows that there are two peaks of the

first oscillator for every peak of the second. The phase portrait has a closed loop which implies that the relative motion of the two oscillators is periodic. The frequencies of the oscillators corresponding to the peaks in the power spectrum are in the ratio $2:1$. The time series and phase evolution plots reveal the highly nonlinear nature of relaxation oscillations.

For a fixed detuning, $\kappa = 0.26$, as the coupling strength is increased starting from zero, the system goes through a cascade of $m:n$ locking regimes as shown in Fig. (3). The frequency ratio, $f_1:f_2$, is plotted as a function of the linear coupling strength, α. The uncoupled frequency ratio is about 3.5 and this ratio decreases with increasing coupling strength. The plateaus in the frequency ratio plot correspond to different regimes of $m:n$ locking and the system goes from $3:1$ to $2:1$ to $1:1$ locking with relatively large plateaus while passing through intermediate locking states such as $5:2, 7:3, 5:3$ etc. with relatively small plateaus. The structure resembles that of a devil's staircase found commonly in limit cycle oscillators that are externally driven by a forcing function. The plot suggests that the presence of non-uniform oscillations, such as those exhibited by relaxation oscillators, promotes higher order locking between oscillators even in the presence of linear coupling.

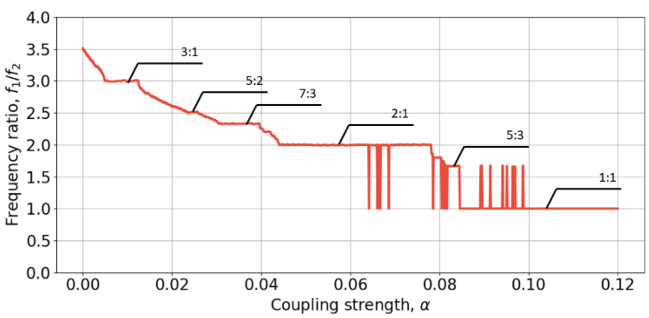

FIGURE 3: $m:n$ locking in a system of two linearly coupled strongly nonlinear Van der Pol oscillators given by Eq. (1). Other $m:n$ integer locks might exist but the finite resolution of the numerical analysis limits the ability to observe them.

We have seen that for the case of linear coupling, $m:n$ locking is not seen in weakly nonlinear Van der Pol oscillators with $\varepsilon = 0.01$ but is present and has a rich structure for the case of strongly nonlinear Van der Pol oscillators with $\varepsilon = 10$. The transition from the weak to strong nonlinear case is of interest and is studied using a parameter sweep of the scaling parameter, $\varepsilon \in (0,10)$ and the coupling strength, $\alpha \in (0,0.15)$. The system of equations is given by Eq. (1). The frequency ratios of the form $n:1$ are shown in Fig. (4). For low values of the scaling parameter, ε, there is no $n:1$ locking observed. Regions corresponding to $2:1, 3:1$ and $1:1$ locking appear for higher values of ε. The boundaries of the $n:1$ locking regions are diffused because of sensitivity to initial conditions and the resolution of the numerical method. Between the regions corresponding to different $n:1$ locks, there are bands corresponding to different frequency ratios $m:n$ that are not shown. The detuning between the oscillators, $\kappa = 0.26$, is kept fixed and changing the detuning parameter will change the structure of the locking regions. In the detuning-coupling space we would expect Arnold tongues corresponding to the various $m:n$ locking regions overlapping for higher values of the coupling strength. It is also worth noting that Fig. (3) corresponds to the projection of the plot in Fig. (4) for $\varepsilon = 10$.

In this section, we noted that higher order $m:n$ locking in coupled Van der Pol oscillators is promoted by the presence of strong nonlinearity and can also be induced by nonlinear coupling terms. In the following sections we focus on introducing nonlinearities in the system via the stiffness terms that arise in micro- and nano- systems in order to study their higher order locking behavior.

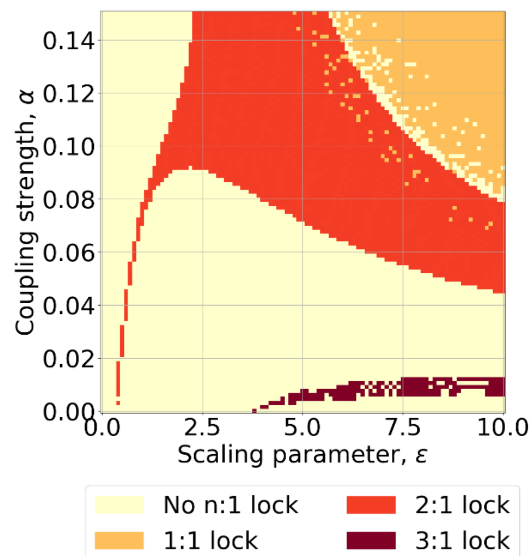

FIGURE 4: $n:1$ locking in a system of two linearly coupled Van der Pol oscillators given by Eq. (1). The plot sweeps the parameters from the weakly nonlinear case to the strongly nonlinear case via the scaling parameter ε. Further, the coupling strength α is varied.

3. SIMPLIFIED MEMS OSCILLATOR SYSTEM

Clamped-clamped beams fabricated from silicon wafers and illuminated by a focused laser beam are known to exhibit non-linearities including stable limit cycle oscillations [11]. A simplified model to describe coupled MEMS oscillators is presented in Eq. (3) that can capture critical properties of such systems and is amenable to analytical treatment [12].

$$\ddot{z} + z = T,$$
$$\dot{T} + T = z(z - p). \tag{3}$$

Here, the dynamical variable z is the displacement of the oscillator while T represents the average temperature of the oscillator. Additionally, the parameter $p > 0$ is derived from the equilibrium position of a corresponding laser-driven MEMS oscillator at minimum laser absorption. The model is a third order system, and the displacement and temperature variables are coupled to each other. In prior work [12], we have shown that this system exhibits a stable limit cycle having amplitude

$\sqrt{10p}/3$. In further developments, we have considered two such oscillators coupled linearly and have charted the bifurcation structure when the two oscillators are identical [12] and detuned [13]. Here we investigate the nature of the coupling more generally.

To study higher order locking we extend the model given in Eq. (3) to a system of coupled oscillators given in Eq. (4). Our primary interest is in 2:1 locking and we choose the uncoupled frequencies of the two oscillators to be close to this ratio. We also include cubic nonlinearity in the oscillators.

$$\begin{gathered}\ddot{z}_1 + z_1 + \varepsilon^2 z_1^3 - \varepsilon T_1 + \varepsilon^2 h(z_1 - z_2) = 0,\\ \dot{T}_1 = -T_1 + z_1(z_1 - \varepsilon p),\\ \ddot{z}_2 + \left(\frac{1}{4} + \varepsilon^2\kappa\right) z_2 + \left(\frac{1}{4} + \varepsilon^2\kappa\right)\varepsilon^2 z_2^3 - \varepsilon T_2 + \varepsilon^2 h(z_2 - z_1)\\ = 0,\\ \dot{T}_2 = -T_2 + z_2(z_2 - \varepsilon p).\end{gathered} \tag{4}$$

Here, $h(z)$ denotes the coupling function, κ is a detuning parameter and ε is a small scaling parameter. We first consider the case where $h(z) = \alpha z$ i.e. linear coupling with scaling coefficient α, where $m{:}n$ locking is not observed in the numerical simulations with small cubic nonlinearity. We verify the numerical result using the method of two variable expansion to generate a slow flow system of equations given by Eq. (5). Here, r_i and θ_i denote the amplitude and phase of the i^{th}oscillator.

$$\begin{aligned}\frac{dr_1}{d\zeta} &= \frac{pr_1}{4} - \frac{9r_1^3}{40},\\ \frac{dr_2}{d\zeta} &= \frac{2pr_2}{5} - \frac{6r_2^3}{5},\\ \frac{d\theta_1}{d\zeta} &= -\frac{7r_1^2}{60} - \frac{p}{4} - \frac{\alpha}{2},\\ \frac{d\theta_2}{d\zeta} &= \frac{691r_2^2}{240} - \frac{4p}{5} - \alpha - \kappa.\end{aligned} \tag{5}$$

The system given by Eq. (5) does not have any fixed point such that $\theta_1 = 2\theta_2 +$ constant, confirming the absence of 2:1 locking. However, in the presence of quadratic coupling i.e., $h(z) = \alpha z^2$, we obtain a different system of slow flow equations given by Eq. (6).

$$\begin{aligned}\frac{dr_1}{d\zeta} &= -\frac{\alpha\sin(2\theta_2 - \theta_1)\, r_2^2}{4} + \frac{pr_1}{4} - \frac{9r_1^3}{40},\\ \frac{dr_2}{d\zeta} &= -\alpha\sin(2\theta_2 - \theta_1)\, r_1 r_2 + \frac{2pr_2}{5} - \frac{6r_2^3}{5},\\ \frac{d\theta_1}{d\zeta} &= \frac{\alpha\cos(2\theta_2 - \theta_1)\, r_2^2}{4r_1} - \frac{7r_1^2}{60} - \frac{p}{4},\\ \frac{d\theta_2}{d\zeta} &= -\alpha\cos(2\theta_2 - \theta_1)\, r_1 + \frac{691r_2^2}{240} - \frac{4p}{5} - \kappa.\end{aligned} \tag{6}$$

For sufficiently high α, this system has a stable equilibrium with $\theta_1 = 2\theta_2 +$ constant which implies the presence of 2:1 locking. This is confirmed by numerical integration and analogous results for a phase-only model are described in a previous work [14].

With strong cubic nonlinearities, however, we find from numerical integration, $m{:}n$ locking in the simplified oscillator pair given by Eq. (7) in the presence of linear coupling. In this case, the scaling parameters γ_1 and γ_2 are used to control the strength of the cubic nonlinearities in the two oscillators. For parameter values $\gamma_1 = 3.5, \gamma_2 = 18, p = 0.1, \kappa = 0.01$, the uncoupled limit cycle frequencies, with $\alpha = 0$, are given by $f_1 = 1.243$ and $f_2 = 0.788$ and are close to a 3:2 ratio.

$$\begin{gathered}\ddot{z}_1 + z_1 + \gamma_1 z_1^3 - T_1 + \alpha(z_1 - z_2) = 0,\\ \dot{T}_1 = -T_1 + z_1(z_1 - p),\\ \ddot{z}_2 + (1/4 + \kappa)z_2 + \gamma_2(1/4 + \kappa)z_2^3 - T_2 + \alpha(z_2 - z_1) = 0,\\ \dot{T}_2 = -T_2 + z_2(z_2 - p).\end{gathered} \tag{7}$$

For the same parameter values but with coupling strength, $\alpha = 0.2$, we find 3:2 locking as shown in Fig. (5) and for the same parameter values but with $\alpha = 0.5$ we observe 1:1 locking. This observation agrees with the results from the previous section that strong nonlinearities promote $m{:}n$ locking in limit cycle oscillators.

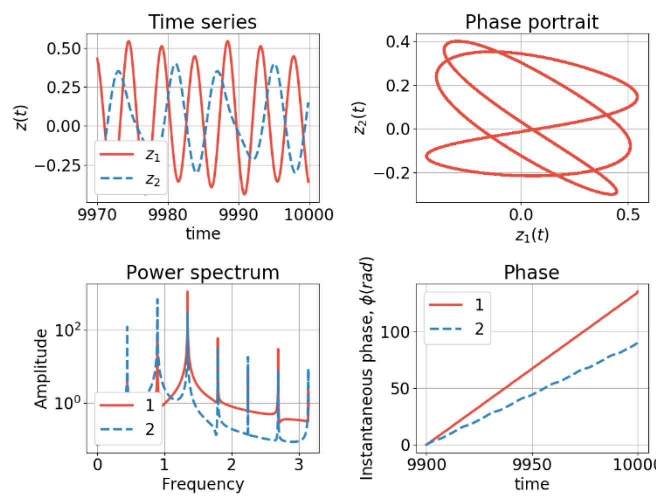

FIGURE 5: 3:2 locking in a system of two linearly coupled strongly nonlinear simplified MEMS oscillators given by Eq. (7). The coupling strength is $\alpha = 0.2$. The locking frequencies are $f_1 = 1.345$ and $f_2 = 0.897$. The phase portrait has a closed loop which implies that the relative motion of the two oscillators is periodic. The frequencies of the oscillators corresponding to the peaks in the power spectrum and the slopes of the instantaneous phase evolution are in the ratio 3:2.

4. THERMO-OPTICAL MEMS OSCILLATOR SYSTEM

The next system of interest describes the oscillations of thermo-optically driven MEMS limit cycle oscillators [15]. The system consists of two clamped-clamped beams that are driven by a continuous-wave laser source of constant power, P_{laser}, that causes the beams to bend in the out-of-plane direction due to thermal effects. Part of the laser is absorbed by the silicon beam and part of it passes through and is reflected from the substrate underneath where it is reabsorbed thus setting up an interferometer cavity and feedback loop that drives the beams into limit cycle oscillations. Sufficiently high laser power is required to set the beams into self-oscillations. Neighboring beams are kept at a voltage difference of V which sets up electrostatic fringing fields between them that result in coupling forces that are modulated by the relative out-of-plane displacement of the oscillators. The equations describing the opto-thermally driven oscillations and interaction of the MEMS beams via electrostatic coupling fields are given by Eq. (8). Beams at the microscopic scale exhibit strong nonlinearities that are represented by the large cubic stiffness factors β. From our discussion so far, we expect higher order frequency locking to be present in this system. Like the previous models the detuning in the system is determined by the parameter κ which is pre-multiplied with both the linear stiffness as well as the cubic stiffness term.

$$
\begin{gathered}
\ddot{z}_1+\frac{\dot{z}_1}{Q}+(1+CT_1)z_1+\beta z_1^3+\frac{V^2(z_1-z_2)}{1+|z_1-z_2|^p}=DT_1,\\
\dot{T}_1=-BT_1+HP_{laser}\left(\alpha+\gamma\sin^2\left(2\pi(z_1-\bar{z})\right)\right),\\
\ddot{z}_2+\frac{\dot{z}_2}{Q}+\kappa(1+CT_2)z_2+\kappa\beta z_2^3+\frac{V^2(z_2-z_1)}{1+|z_2-z_1|^p}=DT_2,\\
\dot{T}_2=-BT_2+HP_{laser}\left(\alpha+\gamma\sin^2\left(2\pi(z_2-\bar{z})\right)\right).
\end{gathered}
\tag{8}
$$

The model parameters are fixed as follows: quality factor $Q=1240$, thermal coefficient for linear stiffness $C=2\times10^{-2}$, cubic stiffness $\beta=15.5$, a fitting parameter $p=2.4$, static displacement per unit change in temperature $D=2.84\times10^{-3}$, thermal constants $B=0.112$ and $H=6780$, laser power $P_{laser}=2\times10^{-3}$, minimum laser absorption $\alpha=0.035$, contrast in absorption $\gamma=0.011$, equilibrium position of the oscillator with respect to the absorption curve $\bar{z}=0.18$. At zero coupling, $V=0$, and frequency detuning, $\kappa=0.14$, the system exhibits limit cycle oscillations with uncoupled limit cycle frequencies $f_1=1.173$ and $f_2=0.532$ with an approximate uncoupled frequency ratio of 2.2. At a coupling strength of $V^2=0.04$, the oscillators lock at an integer ratio of $2:1$ with coupled frequencies, $f_1=1.136$ and $f_2=0.569$. The oscillation information associated with the $2:1$ lock is given in Fig. (6). The nature of oscillations in the MEMS system exhibiting $2:1$ locking is distinguished from that of the Van der Pol system given in Fig. (2) as the MEMS system, even though strongly nonlinear, does not exhibit relaxation oscillations with two distinct timescales. Uniform phase evolution with integer locking is a useful property of the system if the coupled MEMS oscillators are employed as timekeeping devices.

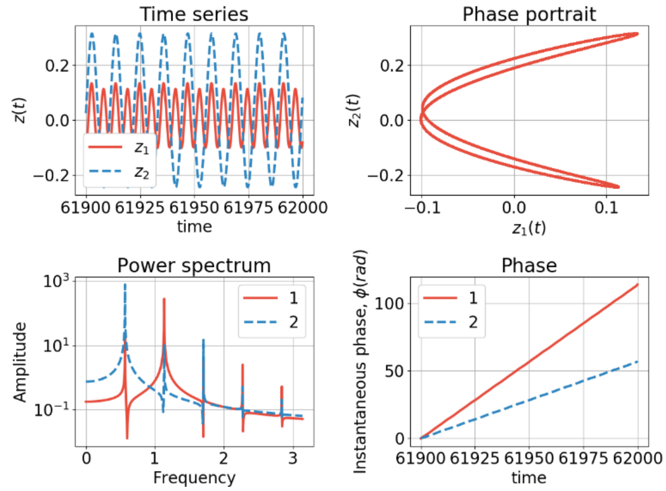

FIGURE 6: $2:1$ locking in a system of two electrostatically coupled thermo-optical MEMS oscillators given by Eq. (8). The time series shows that there are two peaks of the first oscillator for every peak of the second. The phase portrait has a closed loop which implies that the relative motion of the two oscillators is periodic. The frequencies of the oscillators corresponding to the peaks in the power spectrum and the slopes of the instantaneous phase evolution are in the ratio 2:1. The phase evolution is almost linear in time.

2:1 locking exists in the system with strong cubic nonlinearities even when the coupling is made linear or if $C=0$. But when the cubic nonlinearity is suppressed, $2:1$ locking of the oscillators is not observed numerically. A parameter sweep was performed for $\kappa=0.24$, $\beta=0$, $V^2\in[0,0.1]$ and the frequency ratios are plotted in Fig. (7a). In contrast to Fig. (3), there are no plateaus corresponding to $m:n$ locking. This suggests that the term that contributes most to the nonlinearity is the cubic stiffness term and it is essential for achieving $m:n$ lock in the thermo-optical MEMS system. When the calculations are performed with $\kappa=0.14$, and non-zero cubic nonlinearities i.e. with $\beta=15.5$, $2:1$ and $1:1$ locking are observed as shown in Fig. (7b).

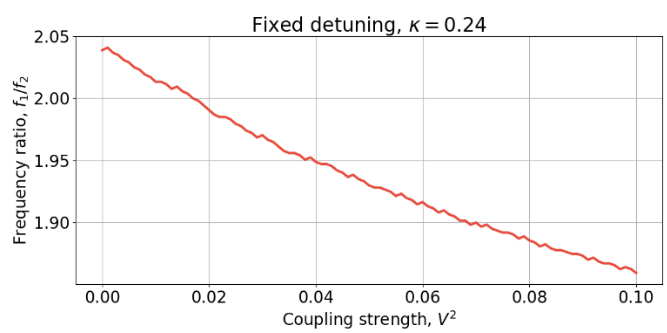

(a)

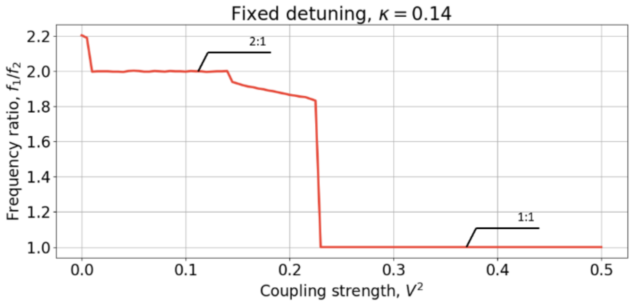

(b)

FIGURE 7: (a) $2:1$ locking is not observed in a system of two coupled thermo-optical MEMS oscillators with cubic nonlinearities suppressed ($\beta = 0$). (b) $2:1$ and $1:1$ locking is observed in a system of two coupled thermo-optical MEMS oscillators with cubic nonlinearities present ($\beta = 15.5$). The oscillator model is given by Eq. (8). There are no intermediate states of $m:n$ coupling between $2:1$ and the $1:1$ coupling regimes.

5. CONCLUSION

Three coupled oscillator models were analyzed for the presence of higher order $m:n$ frequency self-synchronization: the Van der Pol system given by Eqs. (1) and (2), the simplified MEMS oscillator model given by Eqs. (3), (4) and (7), and the thermo-optical MEMS oscillator system given by Eq. (8). In the Van der Pol model, strong nonlinearities which result in relaxation oscillations promote locking in an $m:n$ ratio in the presence of linear coupling. Furthermore, higher order locking in the absence of strong nonlinearities is seen when the coupling is quadratic. In the simplified and thermo-optical MEMS models, strong cubic nonlinearities promote higher order locking in systems with weak linear coupling. The presence of multiple stable $m:n$ lock states for the same detuning levels but for different coupling strengths allows for the possibility of applications such as performing basic computations such as multiplication and division using MEMS oscillator arrays. Future directions of work would involve mapping the Arnold tongues corresponding to each of the $m:n$ locked states in the MEMS oscillator model and explaining the physical intuition behind $m:n$ locking in the case of undriven systems of coupled limit cycle oscillators.

ACKNOWLEDGEMENTS

This material is based upon work supported by the National Science Foundation (NSF), United States under grant number CMMI-1634664.This work used allocation TG-MSS170032 at the Extreme Science and Engineering Discovery Environment (XSEDE), which is supported by NSF, United States grant number ACI-1548562. Specifically, it used the Bridges system, which is supported by NSF, United States award number ACI-1445606, at the Pittsburgh Supercomputing Center (PSC).

REFERENCES

[1] Pikovsky, A., Kurths, J., Rosenblum, M., and Kurths, J. (2003). Synchronization: a universal concept in nonlinear sciences (No. 12). Cambridge university press.

[2] Osipov, G. V., Kurths, J., and Zhou, C. (2007). Synchronization in oscillatory networks. Springer Science & Business Media.

[3] Rosin, D. P., Rontani, D., and Gauthier, D. J. (2014). Synchronization of coupled Boolean phase oscillators. Physical Review E, 89(4), 042907.

[4] Wang, H., Dhayalan, Y., and Buks, E. (2016). Devil's staircase in an optomechanical cavity. Physical Review E, 93(2), 023007.

[5] Singh, H., Konishi, K., Bhuktare, S., Bose, A., Miwa, S., Fukushima, A., Yakushiji, K., Yuasa, S., Kubota, H., Suzuki, Y., and Tulapurkar, A.A. (2017). Integer, fractional, and sideband injection locking of a spintronic feedback nano-oscillator to a microwave signal. Physical Review Applied, 8(6), 064011.

[6] Mirollo, R. E., and Strogatz, S. H. (1990). Synchronization of pulse-coupled biological oscillators. SIAM Journal on Applied Mathematics, 50(6), 1645-1662.

[7] Shukrinov, Y. M., Medvedeva, S. Y., Botha, A. E., Kolahchi, M. R., and Irie, A. (2013). Devil's staircases and continued fractions in Josephson junctions. Physical Review B, 88(21), 214515.

[8] Ermentrout, G. B. (1981). n: m Phase-locking of weakly coupled oscillators. Journal of Mathematical Biology, 12(3), 327-342.

[9] Lingnau, B., Shortiss, K., Dubois, F., Peters, F. H., and Kelleher, B. (2020). Universal generation of devil's staircases near Hopf bifurcations via modulated forcing of nonlinear systems. Physical Review E, 102(3), 030201.

[10] Asadi, K., Yeom, J., and Cho, H. (2021). Strong internal resonance in a nonlinear, asymmetric microbeam resonator. Microsystems & Nanoengineering, 7(1), 1-15.

[11] Aubin, K., Zalalutdinov, M., Alan, T., Reichenbach, R. B., Rand, R., Zehnder, A., Parpia J, and Craighead H. (2004). Limit cycle oscillations in CW laser-driven NEMS. *Journal of microelectromechanical systems*, *13*(6), 1018-1026

[12] Rand, R. H., Zehnder, A. T., Shayak, B., and Bhaskar, A. (2020). Simplified model and analysis of a pair of coupled thermo-optical MEMS oscillators. Nonlinear Dynamics, 99(1), 73-83.

[13] Shayak, B., Bhaskar, A., Zehnder, A. T., and Rand, R. H. (2020). Coexisting modes and bifurcation structure in a pair of coupled detuned third order oscillators. International Journal of Non-Linear Mechanics, 122, 103464.

[14] Keith, W. L., and Rand, R. H. (1984). 1: 1 and 2: 1 phase entrainment in a system of two coupled limit cycle oscillators. Journal of Mathematical Biology, 20(2), 133-152.

[15] Zehnder, A. T., Rand, R. H., and Krylov, S. (2018). Locking of electrostatically coupled thermo-optically driven MEMS limit cycle oscillators. International Journal of Non-Linear Mechanics, 102, 92-100.